Bicyclic helical peptides as dual inhibitors selective for Bcl2A1 and Mcl-1 proteins

Aline D. de Araujo,[†] Junxian Lim, [†] Kai-Chen Wu, [†] Yibin Xiang,[ǂ] Andrew C. Good, [ǂ] Renato Skerlj[ǂ] and David P. Fairlie[†]*

[†] Division of Chemistry and Structural Biology, ARC Centre of Excellence in Advanced Molecular Imaging, Institute for Molecular Bioscience, The University of Queensland, Brisbane, QLD 4072, Australia.

[ǂ] Noliva Therapeutics LLC, Newton, MA 02465, USA.

ABSTRACT

A 26-residue peptide BimBH3 binds indiscriminately to multiple oncogenic Bcl2 proteins that regulate apoptosis of cancer cells. Specific inhibition of the BimBH3-Bcl2A1 protein-protein interaction was obtained in vitro and in cancer cells by shortening the peptide to 14 residues, inserting two cyclization constraints to stabilize a water-stable alpha helix, and incorporating an N-terminal acrylamide electrophile for selective covalent bonding to Bcl2A1. Mass spectrometry of trypsin-digested bands on electrophoresis gels established covalent bonding of an electrophilic helix to just one of the three cysteines in Bcl2A1, the one (Cys55) at the BimBH3-Bcl2A1 protein-protein interaction interface. Optimizing the helix-inducing constraints and the sequence subsequently enabled electrophile removal without loss of inhibitor potency. The bicyclic helical peptides were potent, cell permeable, plasma-stable, dual inhibitors of Bcl2A1 and Mcl-1 with high selectivity over other Bcl2 proteins. One bicyclic peptide was shown to inhibit the interaction between a pro-apoptotic protein (Bim) and either endogenous Bcl2A1 or Mcl-1, to induce apoptosis of SKMel28 human melanoma cells, and to sensitize them for enhanced cell death by the anticancer drug etoposide. These approaches look promising for chemically silencing intracellular proteins.

INTRODUCTION

Tumor cells develop the capacity during oncogenesis to evade regulatory apoptosis by overexpressing prosurvival proteins or downregulating pro-apoptotic signalling pathways. These measures also enable cancer cells to survive DNA-damaging cytotoxic drugs. Apoptosis is regulated by a complex network of proteins, including anti-apoptotic (e.g. Bcl-2, Bcl-xL, Bcl-w, Mcl-1, Bcl2A1) and pro-apoptotic Bcl2 family proteins.[1] The expression and importance of each anti-apoptotic protein varies with cancer cell lineage and tumor stage, and may change during chemotherapy.[1] Therefore, inhibiting one or more of these proteins has the potential to induce apoptosis in different types and stages of cancer.[1]

Pro-apoptotic proteins present their α-helical BH3 domain to a conserved hydrophobic cleft within anti-apoptotic proteins, and this has guided rational design of inhibitors of Bcl2 proteins.[1] These inhibitors have been either peptides modeled after BH3 domains or synthetic small organic molecules, with some validated examples undergoing clinical trials, including ABT-737 and navitoclax (targeting Bcl-2/Bcl-xL/Bcl-w), obatoclax (pan-Bcl2 inhibitor) and venetoclax, a recent FDA-approved drug targeting Bcl-2 in chronic lymphocytic leukemia.[2]

Mcl-1 is a related Bcl2 family protein overexpressed in a variety of human cancers[3] whereas Bcl2A1 (abbreviated A1) is more often upregulated in melanoma, leukemia and lymphoma.[4] Both A1 and Mcl-1 have important roles in melanoma progression.[5-8] Their simultaneous knockdown using siRNA caused death of melanoma cells, while healthy cells were unaffected.[6] Moreover, melanoma resistance to Braf or MEK inhibitors correlated with A1 and Mcl-1 upregulation and was attenuated by neutralizing with siRNA.[5-8] Therefore, new drugs that selectively inhibit both A1 and Mcl-1 proteins might be very promising. Only a few compounds are known to exclusively act on Mcl-1 in cells,[9-11] with a newly discovered small molecule showing promise in clinical studies,[10] while selective A1 modulators are not yet well

developed.[12,13] Compounds that inhibit all Bcl-2 family proteins are known, but recent clinical trials showed that Bcl-xL inhibition can be toxic to platelets so more target selectivity is required.[1b-1d]

The BH3 domain of pro-apoptotic protein Bim (BimBH3 81-106, Figure 1) binds tightly to all anti-apoptotic Bcl2 proteins.[14] Several studies have used either computational modelling, single point mutation or phage display library screening to identify possible ways to obtain BimBH3 analogues with specificity over different Bcl2 family proteins. [12,15-19] When searching for A1/Mcl-1 exclusive peptide epitopes, a 26-mer peptide Bim_S2A (L62A/F69A) was shown to be selective for Mcl-1,[17] while a 23-mer BimBH3 peptide derivative encompassing 4 mutations was found to bind selectively to A1.[12] Such linear peptides are prone to rapid metabolic degradation and low cell membrane permeability, preventing their clinical use. To overcome this limitation, a hydrocarbon crosslinker was inserted previously into BimBH3 (generating 21-mer pan-Bcl2 inhibitor $BimSAHB_A$, Figure 1), in a chemical approach known as stapling, that stabilized the α-helical conformation of the peptide and allowed its cell uptake by cancer cells inducing apoptosis.[20] With five residues removed from the N-terminus of BimBH3, $BimSAHB_A$ nevertheless binds promiscuously to all anti-apoptotic Bcl-2 proteins. To our knowledge, there are no reports describing cell permeable Bim-peptide variants selective for A1 and Mcl-1, but a modified stapled BimBH3 peptide was recently shown to bind exclusively to Mcl-1 and to induce death of Mcl-1 dependent cells .[21]

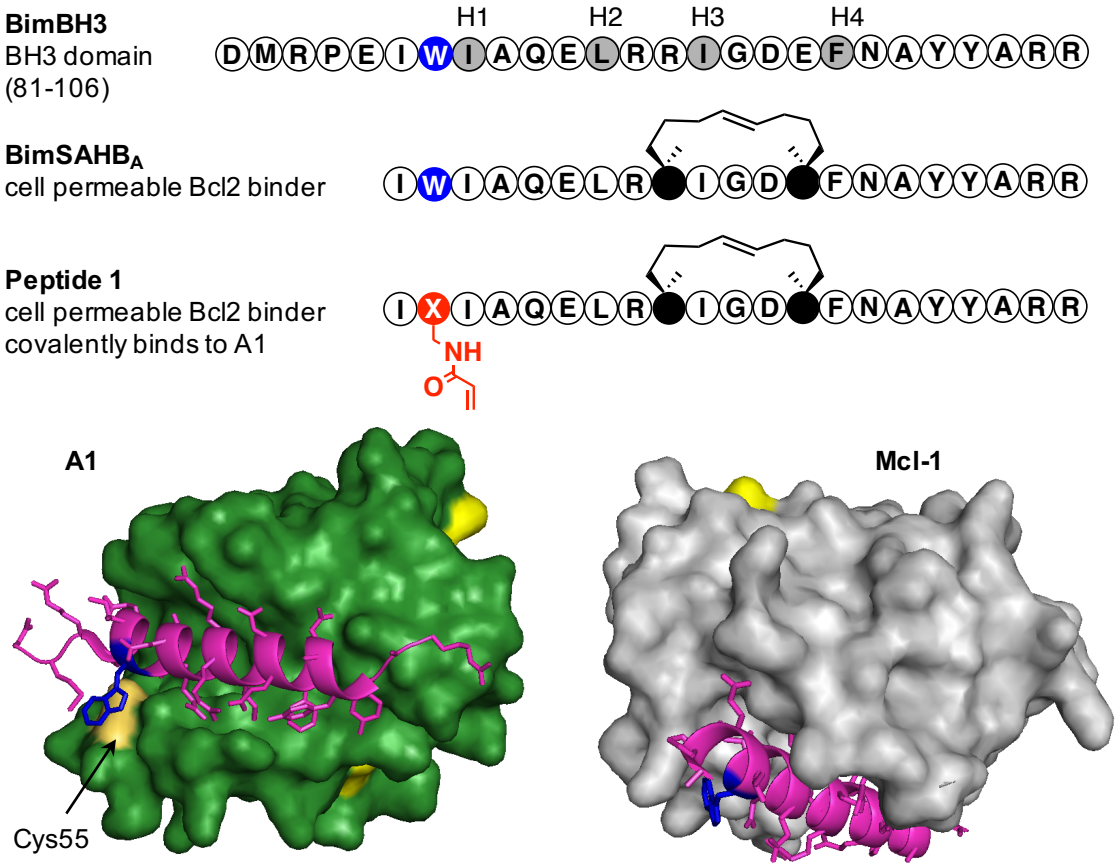

Figure 1. BimBH3 (pink) interacts with all anti-apoptotic Bcl2 proteins, including A1 (green, PDB 2vm6) and Mcl-1 (gray, PDB 2nl9) by presenting four conserved hydrophobic residues (H1-H4) on one helical face to the BH3 groove. When equipped with a helical-inducing hydrocarbon crosslinker (BimSAHB$_A$), BimBH3 can enter into cancer cells and trigger apoptosis.[20] When the native Trp2 in BimSAHB$_A$ (blue) is modified with an electrophilic residue (red) to form peptide **1** (X= Dap-*N*-acrylamide), exclusive covalent bonding to a uniquely positioned cysteine in A1 (Cys55) takes place, without interaction with other exposed cysteines on the surface of A1 or other Bcl2 proteins (cysteines in yellow).[22]

We[22,23] and others[24] recently reported a strategy for potently inhibiting Bcl2A1 by covalently bonding BimBH3 peptides to a distinctive cysteine (Cys 55) located in the BimBH3-binding site in A1 (Figure 1). This cysteine is not present in the BH3 binding site of other anti-apoptotic Bcl2 proteins.[22,24] Our approach utilized an acrylamide as an electrophilic warhead which was incorporated at position 2 in BimSAHB$_A$ (e.g. peptide **1** in Figure 1) and was found to selectively and covalently bond *in vitro* through Michael addition to Cys55 in A1,[22] but not to two other cysteines located on the exposed surface of A1. This afforded a cell-penetrating stapled peptide that covalently targeted A1 in living cells.[22,24a] Although affinity to A1 was enhanced in this way, peptide **1** can still interact non-covalently with other Bcl2 proteins, including Bcl-xL.[20] Here we describe further development of helical peptide ligands for A1, using electrophilic analogues for structure-activity optimization, culminating in a potent inhibitor of A1 and Mcl-1 that does not bind to other Bcl2 family proteins.

RESULTS AND DISCUSSION

Design of bicyclic helical peptides. Although interacting residues are distributed all along the BimBH3 peptide sequence, molecular dynamics and mutagenesis studies suggested to us that its C-terminal region may be less important for binding to A1 and Mcl-1 than to other Bcl2 proteins.[15-18] Therefore we sought to downsize $BimSAHB_A$, which indiscriminately binds to all Bcl2 proteins, in order to investigate whether shorter peptides could bind selectively to A1 or Mcl-1. These peptides must also penetrate cells to inhibit Bcl2 function in mitochondria. Flow cytometry is normally used to measure cell uptake, but requires tagging helical peptides with bulky hydrophobic fluorescent probes[25] that can themselves artificially promote cell uptake. To remove this possibility, we instead equipped our peptides with a small acrylamide warhead at position 2 (Figure 2). This permitted covalent bonding to A1 in cells, readily detected using western blot as previously observed with peptide **1**.[22] In this way, we could verify whether new peptides enter cells, escape endosomes and interact with endogenous Bcl2 proteins located in the mitochondria.

Among shorter peptides that we synthesized was peptide **2**, with the last seven C-terminal residues from **1** removed to produce a 14-residue peptide featuring a hydrophobic helix-inducing constraint and an acrylamide electrophile at position 2 (Figure 2). Using circular dichroism spectroscopy, we found that α-helicity in aqueous media was significantly reduced upon truncating **1** (74%) to **2** (47%), consistent with depletion of helix-favoring residues (e.g. Ala16, Ala19, Arg20, Arg21). To increase α-helicity, we incorporated a second (*i*, *i* + 4) sidechain to sidechain crosslink at different positions (not shown), eventually settling on a crosslink between residues 1 and 5 as being optimal (Figure 2). A second macrocycle-forming hydrocarbon crosslink in **3** resulted in higher α-helicity than **2** in water (containing 20% acetonitrile for

solubility). Next we varied the two crosslinks (**3-6**, Figure 2) featuring hydrocarbon and/or lactam bridges. Incorporating a second cycle significantly increased α-helicity for the 14-mer peptides, with two hydrocarbon bridges (**3**) being less helical than one hydrocarbon and one lactam (**4**, **5**), while two lactams (**6**) conferred the most α-helicity. This is consistent with published studies on model peptides, where a KD lactam linker induced the greatest peptide α-helicity in water.[26,27] Although less α-helix inducing, highly hydrophobic, hydrocarbon crosslinks can be used to promote greater cell permeation in some stapled peptides, including $BimSAHB_A$ and **1**.[20,22,25]

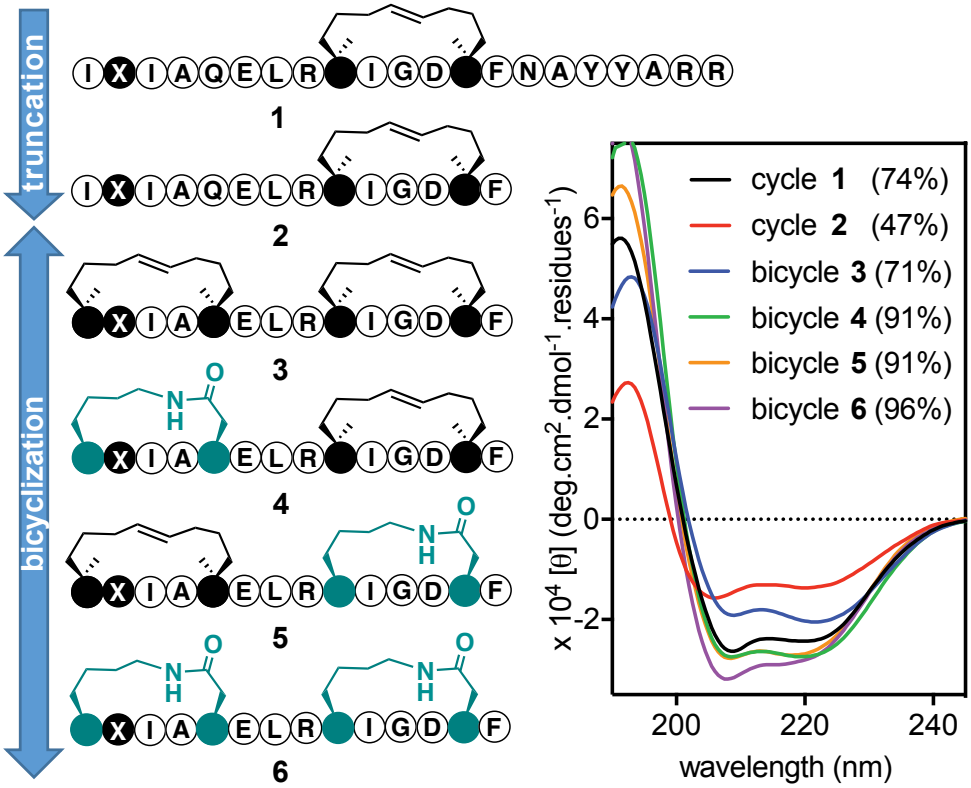

Figure 2. Structure of 14-mer peptides **2-6**, derived from **1**, featuring one or two crosslinking bridges. *Right*: CD spectra of **1-6** (50 μM) in 20% acetonitrile in water. Percent helicity is in parenthesis. X= Dap-*N*-acrylamide. All peptides are acetylated at the N-terminus and amidated at the C-terminus.

Synthesis of the bicyclic compounds. Peptides were prepared on solid support using standard Fmoc-based solid-phase peptide synthesis (SPPS), followed by on-resin intramolecular lactamization of a Lys(Mtt) and Asp(OPip) pair[26,27] and, when appropriate, ring-closing metathesis between of two *S*-2-(4′-pentenyl)alanine (S5) residues[25] using Grubbs catalyst.[28] Finally, the orthogonal protecting group of Dap2 was removed, allowing incorporation of the acrylamide electrophile. Scheme 1 illustrates the synthesis of peptide **5**. For other peptides, see Figure S1.

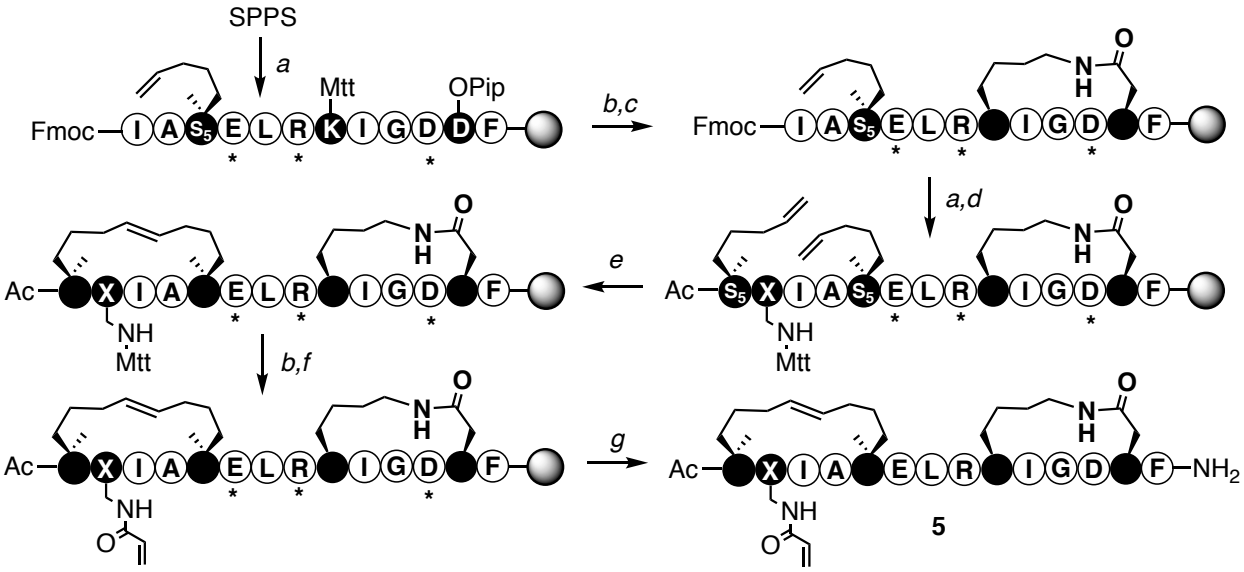

Scheme 1. Synthesis of bicycle **5**. Conditions: a) i. 30% piperidine in DMF, 3 min (2x); ii. Fmoc-AA-OH (4 equiv), HCTU (4 equiv), DIPEA (8 equiv) in DMF, 30 min (2x); b) 2% TFA in DCM, 10 min (10x); c) PyBOP (4 equiv), DIPEA (8 equiv) in DMF, 6h; d) i. 30% piperidine in DMF, 3 min (2x); ii. Ac_2O (1 M), DIPEA (0.4 M) in DMF, 5 min (2x); e) 10 mM Grubbs catalyst 1st generation in dry DCE, 2h (2x); f) acrylic acid (4 equiv), HATU, (4 equiv), DIPEA (4 equiv) in DMF, 15 min; g) TFA:TIS:H_2O (95:2.5:2.5), 2h. Asterisks indicate use of standard protecting groups.

Binding to Bcl2 proteins. Next we measured binding to different Bcl2 proteins (Figure 3) using a fluorescence polarization (FP) assay to observe competition of these new peptides (**2-6**) with a fluorescein-labelled Bid ligand (FBid).[22] BimBH3 (86-106, **BIM**) and **1** were compared as controls. Because acrylamide-bearing peptides **1-6** bind covalently to A1, the FBid/A1 inhibitory curves varied over time (Figure S2). The kinetics of the binding are discussed in the next section. Here we selected the 2 h incubation time point to compare A1 binding and reported the experimental A1-binding parameters as IC_{50}(2h) and K_i(2h) for each peptide **1-6** (Figure 3).

After 2 h incubation, the bicyclic peptides **3-6** bound more tightly than the monocyclic **2** or the longer sequences (**BIM** and **1**) to A1 (Figure 3A) and Mcl-1 (Figure 3B), with peptide **5** being the most effective dual binder to these proteins. These results highlight the advantages in target selectivity of stabilizing the N-terminal region with a second helix-inducing constraint. We also investigated the effect of truncation and cyclization in the Bim sequence on binding to other Bcl2 proteins, using similar competition binding experiments (Figure 3C, K_i for Mcl-1, Bcl-2, Bcl-xL and Bcl-w; and K_i(2h) for A1 values in Table S1). As anticipated, C-terminal truncation of **1** to form **2-6** led to significant decreases in binding affinity for Bcl-w, Bcl-xL and Bcl-2, while still preserving nM affinity for Mcl-1 and A1.

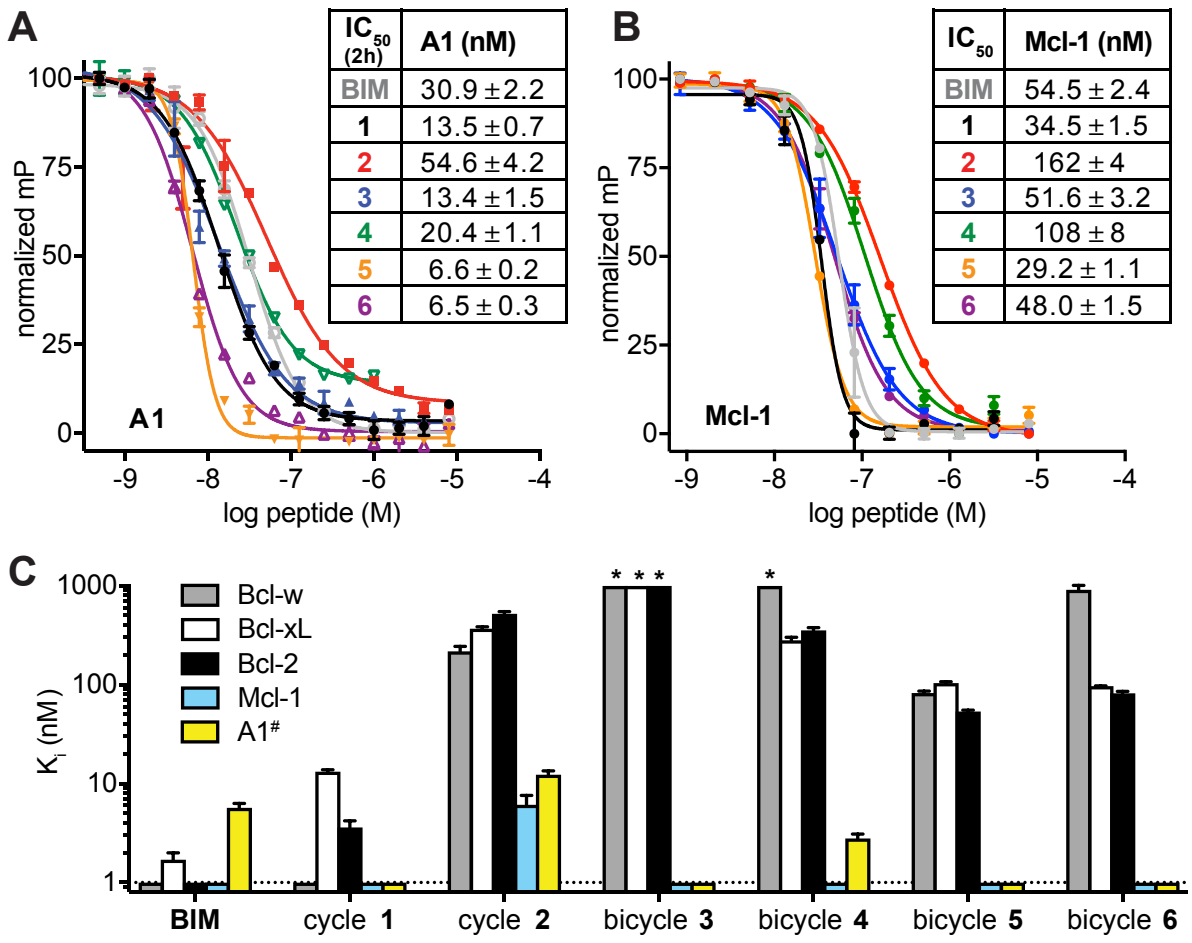

Figure 3. Binding of peptides **BIM** and **1-6** to Bcl2 anti-apoptotic proteins measured by competitive FP assays against a Bcl2 protein/FBid complex after 2 h incubation. **A, B)** Inhibitory curves measured after 2 h incubation of peptides with A1/FBid (15/5 nM) (A) or Mcl-1/FBid (200/20 nM) (B) complex. IC_{50} values determined from FP curves are given in adjacent tables; for A1, IC_{50} values are defined as $IC_{50}(2h)$ given the time-dependence of covalent binding; for Mcl-1, IC_{50} values are at equilibrium. **C)** Comparative K_i values (nM) for binding to all anti-apoptotic Bcl2 proteins. K_i values below the dotted line were < 1 nM and below assay detection. * K_i > 1000 nM. #For covalent binders to A1, K_i values are defined as $K_i(2h)$ given the time-dependence of covalent binding.

Covalent bonding to A1 protein *in vitro*. Covalent bonding of the acrylamide-peptides to A1 gives further insights into binding of the truncated peptides to protein. The binding is time-dependent, as expected for a covalent inhibitor (Figure 4A). We used the second-order rate constant k_{inact}/K_I to describe the efficiency of covalent bond formation, accounting for both the potency of the first step related to affinity (K_I) and the maximum rate of covalent bond formation (k_{inact}) (Figures 4B and 4C).[29]

The best fitting peptides to the binding groove likely position the acrylamide electrophile precisely for interaction with Cys55 in A1, facilitating nucleophilic attack and rapid covalent bonding. Positioning a lactam bridge near the C-terminus led to faster binding (**5** and **6**), attributed to greater helix induction in this region and better conformational preorganization of the peptide for protein binding. The presence of a hydrocarbon linker near the N-terminus increased binding, as reflected by a 3-fold higher K_I for bicycle **5** in comparison to **6** (Figure 4). Overall, bicycle **5** was the most efficient covalent binder. All acrylamide-peptides efficiently attached to A1 after 2 h, as assessed by SDS-PAGE electrophoresis (Figures 5A and S3) and mass spectrometry (Figures 5B and S4) and only a 1:1 conjugate with A1 was observed, consistent with selective covalent bonding to one site only on the protein. The specific site of covalent attachment was established for **5** by digesting the protein-peptide conjugate band from the gel with trypsin and performing MS/MS analysis (Figure 5C and S5). No peptide herein bonded covalently with the other Bcl2 proteins (not shown) consistent with no active site Cys in those proteins. Peptides with no warhead such as **BIM** and bicycle **7**, an analogue of **5** with acrylamide replaced by a non-electrophilic propionamide isostere (Figure 7A), showed no covalent bonding to A1 (Figure 5B).

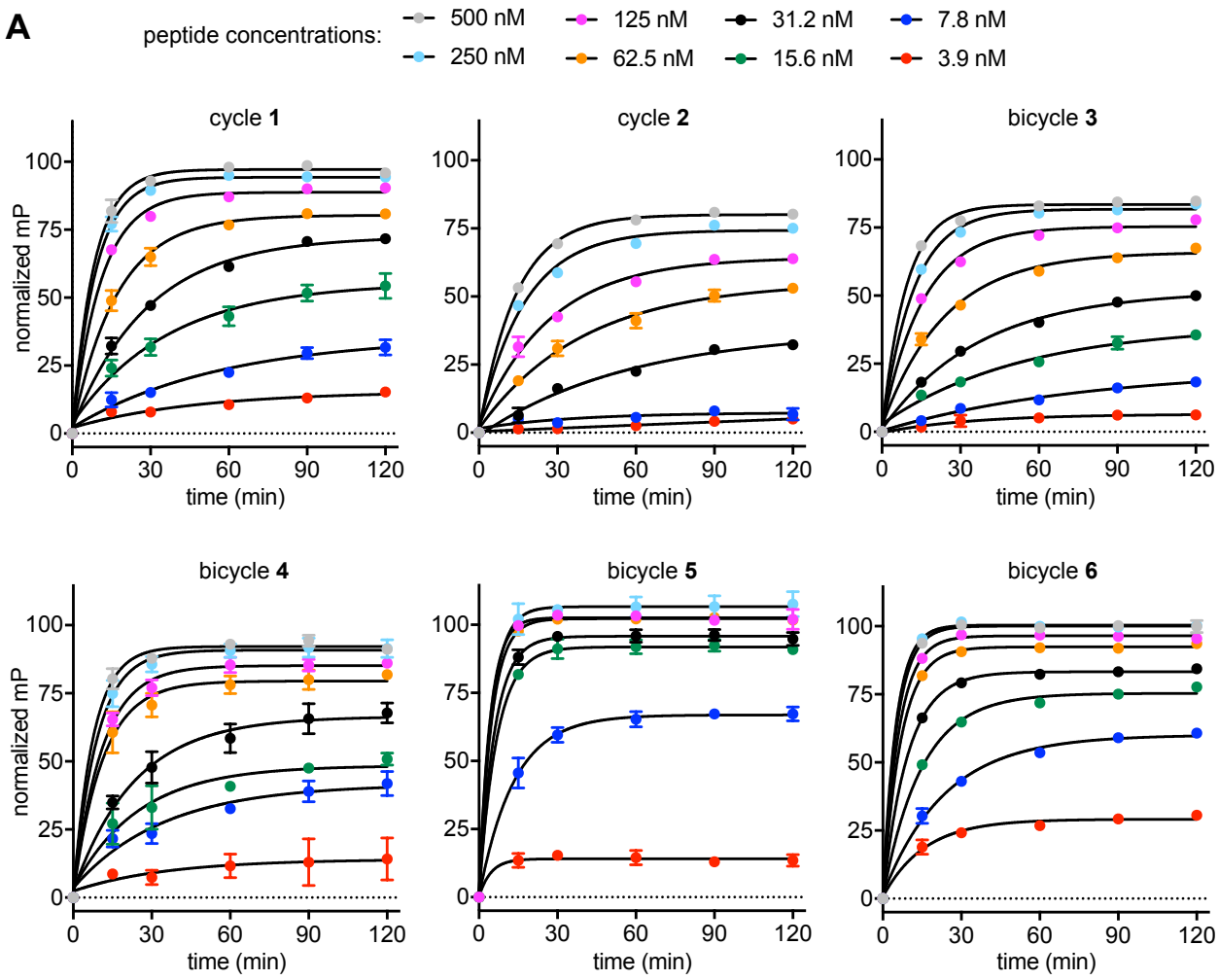

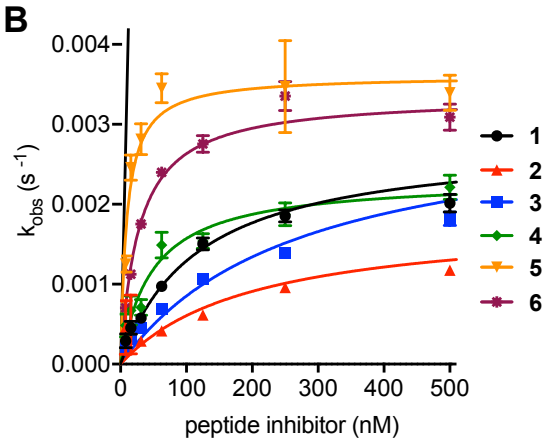

C

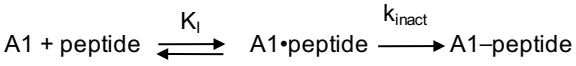

Peptide	K_I (nM)	k_{inact} (ms^{-1})	k_{inact}/K_I ($mM^{-1}.s^{-1}$)
1	81.6 ± 10.8	2.39 ± 0.11	30.0 ± 5.3
2	175 ± 26	1.59 ± 0.10	9.0 ± 1.6
3	133 ± 19	2.24 ± 0.13	16.2 ± 2.3
4	46.7 ± 12.0	2.31 ± 0.17	54.0 ± 17.5
5	10.0 ± 2.6	3.67 ± 0.20	399 ± 124
6	30.5 ± 4.2	3.49 ± 0.13	118 ± 20

Figure 4. Kinetics of covalent binding of acrylamide-containing peptides **1-6** to A1. **A)** Inhibition of the A1/FBid (15/5 nM) complex changed over time for each peptide concentration used ([peptide] = 500, 250, 125, 61.5, 31.2, 15.6, 7.8 and 3.9 nM). The change in polarization over time (t) was fitted to the equation: normalized % polarization = 100*(1 - exp(-k_{obs}*t)), to

determine k_{obs}, the observed rate of inactivation for each peptide concentration. **B)** The k_{obs} values are then used to determine the parameters k_{inact} and K_I by plotting the curve: $k_{obs} = k_{inact}*[peptide]/(K_I + [peptide])$. **C)** Overall, the covalent peptides associate to A1 via a two-step mechanism: first peptide binds reversibly to A1 with potency reflected by K_I values; then irreversibly attaches to A1, with maximum k_{obs} defined as k_{inact}. The k_{inact}/K_I rate describes the overall efficiency of conversion of free A1 to the covalent A1-peptide complex.[29]

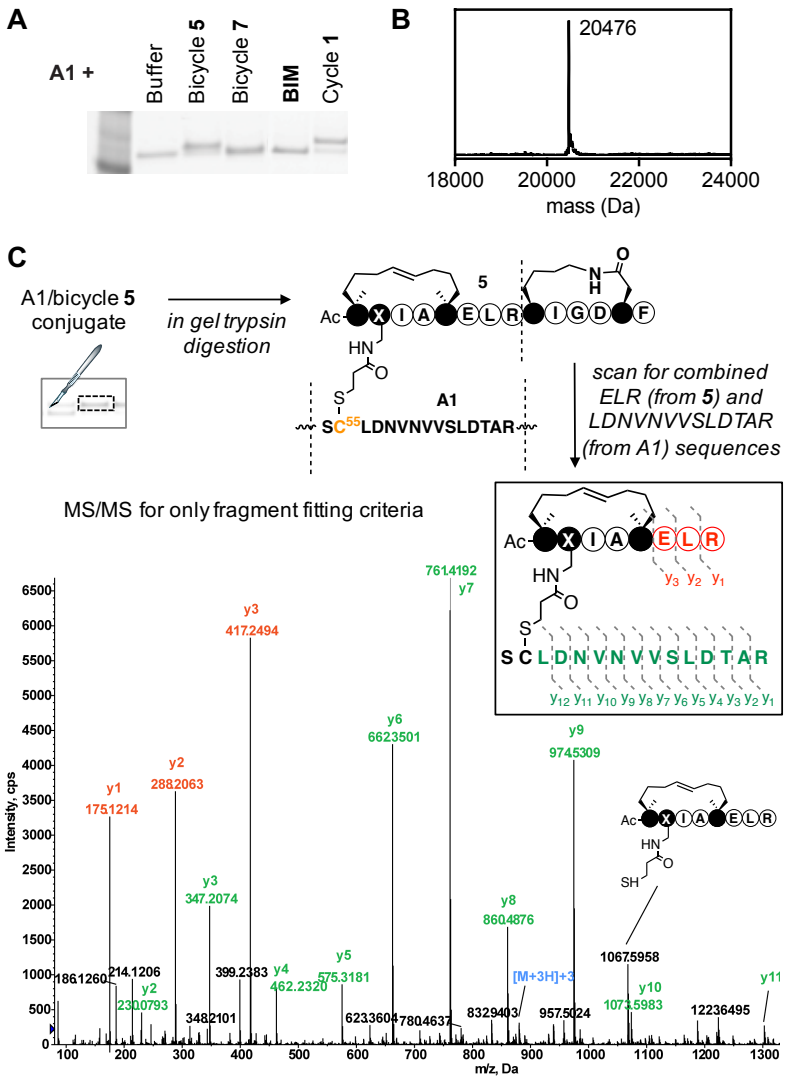

Figure 5. Analysis of covalent bonding of acrylamide-appended peptides to A1 *in vitro*. **A)** Denaturing SDS-PAGE analysis shows that acrylamide-containing peptides (**5** and **1**) covalently

bond to A1, whereas those without warhead do not (**BIM** and **7**). **B)** Mass spectrum of the A1/peptide **5** conjugate formed after incubating A1 (1 μM, MW: 18786) with **5** (10 μM) for 2 h in buffer (pH 7.2), showing the expected molecular weight increment (MW: 20475). No evidence of multiple additions of the peptide to the protein was found. **C)** Mass spectrum analysis of the trypsin-digested gel band, containing the A1 protein fragment bearing Cys55 and covalently bound peptide **5**. The MS/MS fingerprint for m = 2638.30 ($[M+3H]^{3+}$ = 880.8) revealed the expected y ion fragmentation pattern for the A1 derived-sequence LDNVNVVSVDTAR and the peptide **5** derived-sequence ELR (Figure S5). Conjugation of ELR to other protein fragments was not detected, confirming Cys55 to be the only site of covalent peptide attachment.

Covalent bonding to A1 protein in cells. To learn whether the peptides could penetrate cells and covalently bond to intracellular endogenous A1, they were incubated with live U937 lymphoma cells for 24 h. Intracellular A1 was analysed by western blot for modified molecular weight due to covalent bonding with peptide (Figure 6). Like compound **1** (IC_{50} ~ 25 μM),[22] each of the compounds **2-6** did form a covalent adduct consistent with reaction of the electrophile with A1. Bicycle **5** (IC_{50} 1-5 μM) was the most effective covalent ligand, while bicycle **6** that had similar affinity as **5** for A1 protein *in vitro* was less effective in U937 cells, presumably because of lower cell permeability due to no hydrophobic linker. Bicycle **4**, an analogue of **5** with the positions of the lactam and hydrocarbon bridges swapped around, also exhibited a high level of intracellular A1 targeting. Interestingly, the double hydrocarbon-crosslinked peptide **3** was not as an efficient covalent inhibitor in live cells as the mixed-bicyclic constructs **4** and **5**. Bicycle **7** with no electrophile showed no covalent bonding to A1.

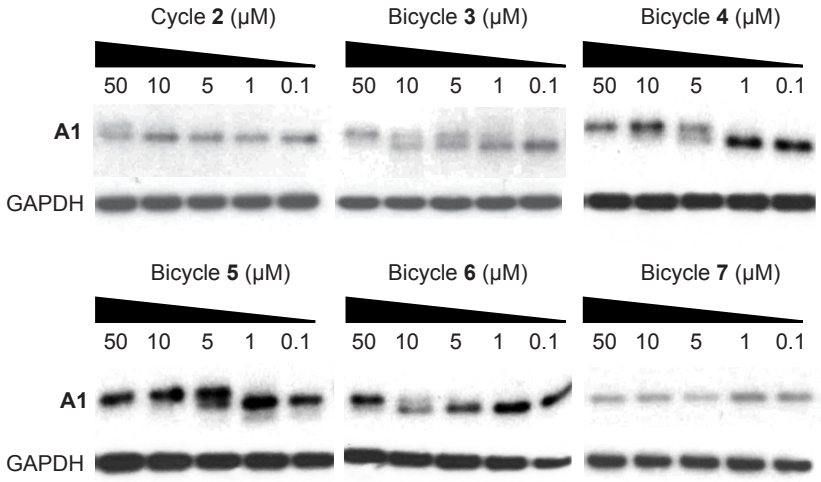

Figure 6. Western blots show concentration-dependent covalent bonding of intracellular A1 to peptides with acrylamide (**2-6**), but not without (**7**), in live cells. U937 cells were incubated with peptides (24 h, 37 ^{0}C) then lysed and analyzed by western blot.

Overall, bicycle **5** was the most efficient binding ligand to A1 and Mcl-1 *in vitro* and to A1 in live cells. Moreover, **5** was a very stable helical scaffold with higher resistance to proteolytic and serum degradation than the parent BimSAHB$_A$-derivative **1** (Figures S6 and S7). Although BimSAHB$_A$ displays enhanced resistance to serum degradation in comparison to the parent linear BimBH3, residues located at the C-terminus of BimSAHB$_A$ are less protected by stapling and more vulnerable to cleavage by proteases (Figure S7). Peptide **3** was the most selective for A1/Mcl-1, but it did not target A1 in cells as well as **5**, suggesting an inferior capacity to reach the cytosol. The synthetic yield for **3** was also poorer, making this peptide less attractive for further investigation.

Non-covalent A1/Mcl-1 dual inhibitor. Having optimised the series to compound **5** as the best covalent ligand for inhibiting A1 and Mcl-1 proteins, we removed the acrylamide electrophile and replaced it with the isosteric propionamide to produce analogue **7** (Figure 7A). Compound **7** was a reversible non-covalent inhibitor with high affinity for A1 and Mcl-1, suggesting that the other changes to the peptide had compensated for the effect of an electrophile resulting in high recognition of the A1 and Mcl-1 binding pocket (Figure 7B and Table S1). Changing the acrylamide (**5**) to propionamide (**7**) did not affect hydrophobicity or structure, as reflected by identical HPLC retention times, CD measured helicity, and similar binding to other Bcl2 proteins (Figure 7B). To potentially improve selectivity for Mcl-1/A1, we replaced Glu with Leu at position 6, a change previously reported to weaken interaction of BimBH3 with Bcl-2, Bcl-w or Bcl-xL proteins. Fluorescence polarization competitive binding measurements demonstrated that bicycle **8** (Figure 7A) had substantially reduced affinity for Bcl-w and Bcl-xL, while maintaining affinity at low nanomolar concentrations for Mcl-1 and A1 (Figure 7B). A fluorescein-labelled analogue of bicycle **8**, peptide **9** (Figure 7A)**,** was synthesized to measure direct binding to the proteins and confirm this selectivity. Indeed, **9** did have affinity at low nanomolar concentrations for both A1 and Mcl-1, but with 50-1000 fold selectivity over other Bcl2 proteins (Figure 7C). Peptide **9** was also examined for cell permeation using flow cytometry, establishing that construct **8** was cell permeable (Figure 8A). Additionally, western blot analysis of an acrylamide derivative of **8**, peptide **10**, revealed similar covalent bonding as bicycle **5** to intracellular A1 (Figure S8).

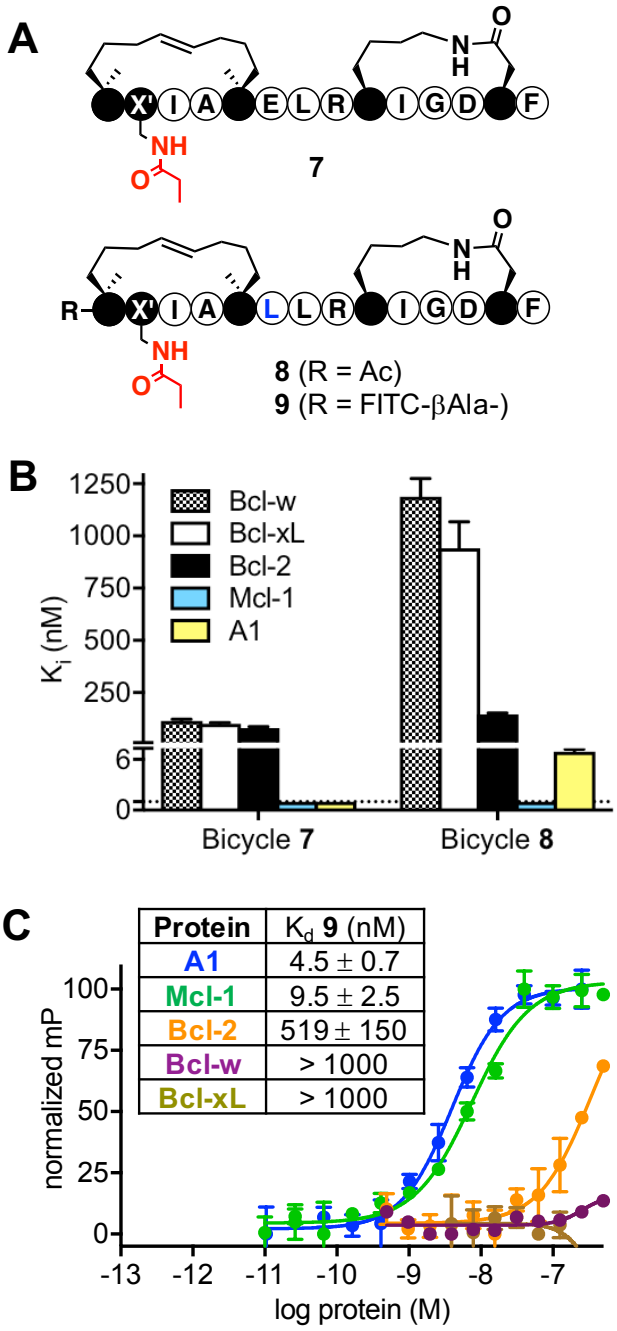

Figure 7. A) Structure of bicyclic peptides **7**, **8** and **9** with no electrophile. X'= Dap-*N*-propionamide. **B)** Comparison of K_i values (nM) for binding of **7** and **8** to five anti-apoptotic Bcl2 proteins. K_i values below the dotted line were < 1 nM. **C)** Direct FP assays displaying binding affinity of the FITC-derived peptide **9** (10 nM) to the Bcl2 proteins. The K_d values determined from the binding curves for each Bcl2 protein are listed in the table.

To evaluate the ability to induce apoptosis of human melanoma cells, we incubated bicycle **8** with SKMel-28 melanoma cells, which express Mcl-1 and A1 and are reportedly sensitive to Mcl-1/A1 protein silencing.[5-8] Using an MTT assay, we observed that bicycle **8** reduced SKMel28 cell viability in a dose-dependent manner (IC_{50} 8.8 μM) after 48 h incubation (Figure 8B), more potently than the parent $BimSAHB_A$ (IC_{50} 15.7 μM, Figure S9). The observed cell death was not caused by nonspecific cytotoxicity via cell membrane lysis, as an LDH release assay confirmed no cell lysis even in the presence of 50 μM peptide (Figure 8C). To correlate the observed decrease in cancer cell viability with intracellular A1/Mcl-1 targeting, we analyzed the association of pro-survival proteins A1 and Mcl-1 with pro-apoptotic protein Bim in SKMel28 cells, using anti-Bim immunoprecipation (IP). As depicted in Figure 8D, bicycle **8** was capable of blocking the interaction of either A1 or Mcl-1 with endogenous Bim. Next we evaluated the capacity of bicycle **8** to sensitize SKMel28 cells to apoptosis induced by chemotherapeutic drugs. As shown in Figure 8E, peptide **8** exhibited a synergistic effect with the drug etoposide, with the combination of both agents enhancing cell death.

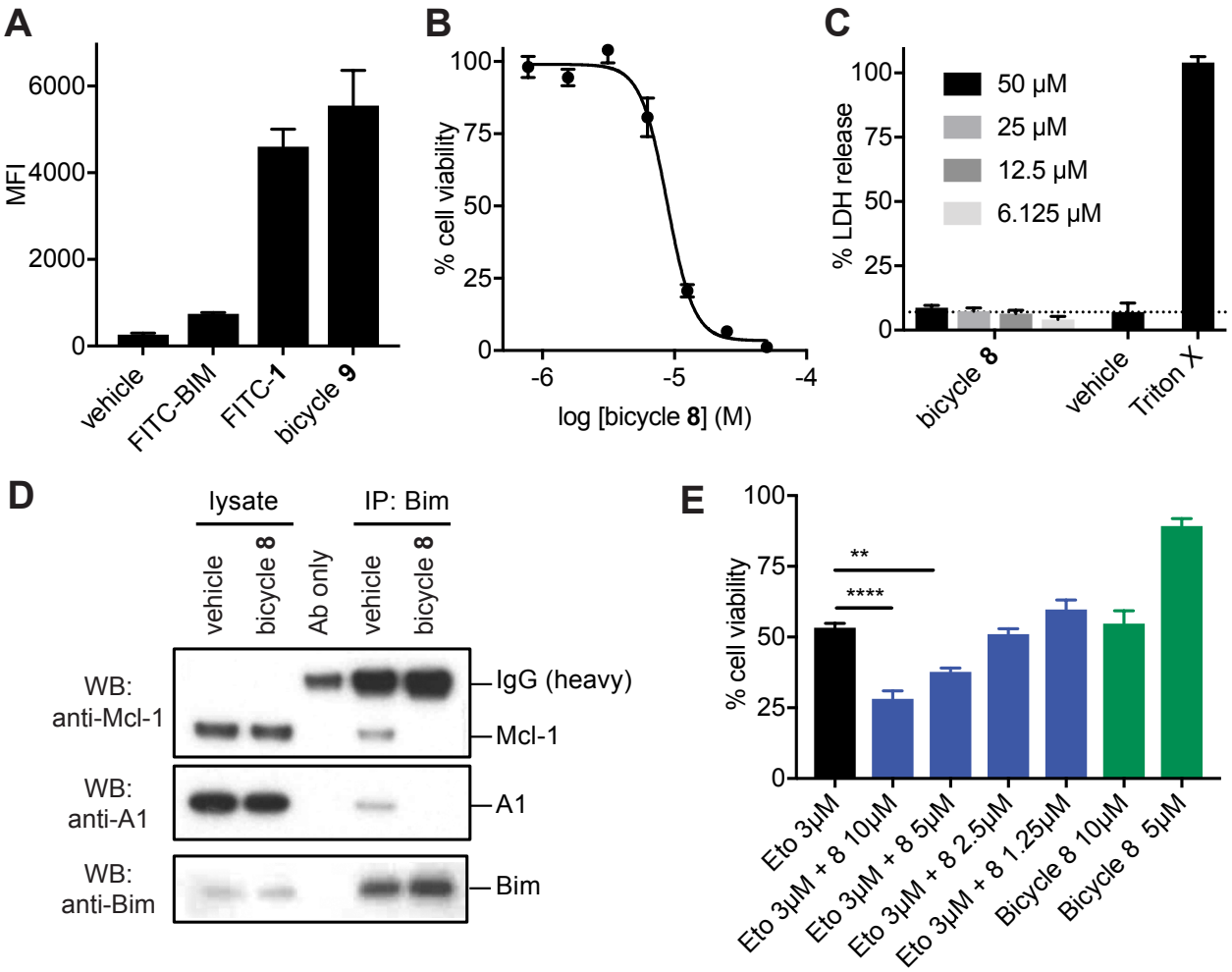

Figure 8. Activity of bicyclic helix **8** (no electrophile) in SKMel28 melanoma cells. **A)** Flow cytometry shows cell uptake of bicyclic helix **9** (FITC-**8**) at similar concentrations as 21mer fluorescein-labelled **1** (FITC-**1**). Linear FITC-**BIM** was a control with negligible cell permeability. **B)** Cell viability after incubation with **8** for 48 h. **C)** LDH release after incubation of SKMel28 cells with **8**. **D)** Bicycle **8** blocked binding of endogeneous pro-apoptotic Bim to Mcl-1 and A1. SKMel28 cells were treated with **8** (30 µM) for 24 h and immunoprecipitation were performed for Bim. Cell lysate and eluted immunoprecipitated (IP) proteins from beads were western blotted for Mcl-1 and A1 proteins. **E)** Cell viability after incubation with etoposide (black) or **8** (green) or both (blue) for 48 h.

CONCLUSIONS

In conclusion, we have developed short helical bicyclic Bim-derived peptides as potent dual inhibitors of Bcl2A1 and Mcl-1, with selectivity over other Bcl-2 family proteins. These compounds were shown to penetrate lymphoma and melanoma cells expressing Bcl2A1 and Mcl-1. One of these compounds, optimized for Bcl2A1 and Mcl-1 binding, was shown to induce apoptosis of human SKMel28 melanoma cells. A series of chemical changes were made to the 26-residue BimBH3 peptide, which indiscriminately binds all Bcl2 proteins. The modifications were: (i) truncation to a 14-residue sequence by removing multiple N- and C- terminal residues; (ii) strategic incorporation of two helix-inducing constraints, one C-terminal KD lactam bridge to induce stronger α-helicity and one N-terminal hydrocarbon crosslink to aid cell penetration; and (iii) a Glu-to-Leu substitution to increase A1/Mcl-1 selectivity and hydrophobicity and cell uptake. These modifications led to helical bicyclic peptide **8**, a novel cell-permeable A1/Mcl-1 inhibitor with higher resistance to proteolytic degradation and more binding selectivity over other Bcl2 family proteins than BimBH3 or BimSAHB$_A$ (Figure 7). These compounds add to our growing library of novel bicyclic peptidomimetics.[30,31]

We have previously shown that a peptide helix with an acrylamide warhead can bond covalently and selectively to a specific cysteine in the protein A1.[22] This could be a valuable approach to silencing proteins and prolonging the *in vivo* action of peptide drugs in particular, since high clearance rates usually shorten the duration of action of peptides. In this paper we have instead focused on using a small electrophile appendage as a tool to permit observation of an intracellular covalent peptide-A1 adduct in live cells, which is otherwise not detectable. We did detect intracellular targeting of the electrophilic peptides to mitochondrial A1, assisting optimization of the peptide sequence for target selectivity and cell activity. This approach is different from conventional tagging with bulky hydrophobic fluorophores that can distort

assessments of cell permeability. First, the acrylamide is small and less likely to interfere with ligand structure and chemical properties than bulky hydrophobic fluorophores. Second, it shows whether the ligand is capable of reaching its cytosolic target, without being influenced by hydrophobic fluorophores. Third, the use of covalent bonding electrophiles aids optimization of other ligand components for enhanced affinity for the target protein but, once optimized, can potentially be removed. For example, it was traditional for many years to use an electrophile in serine protease inhibitors to confer high potency but, once other components of the covalent ligand were optimized, sometimes the electrophile could be removed to leave highly potent non-covalent inhibitors.[31] Similarly we were able to derive bicyclic helical peptide **8**, without electrophile from inhibitor **5** with electrophile. Due to their unique Mcl-1/A1 selectivity, bicyclic helical compounds **5**, **7** and **8** could potentially be useful mechanistic tools for investigating the biological implications of Mcl-1 and A1 dual inhibition *in vivo* and enable further development of a peptide drug to induce apoptosis in cancer cells expressing those proteins.

In a more general context, the combination of shortening helical peptides using back-to-back cyclisation constraints, together with incorporating an electrophile for covalent binding, represents a powerful new approach to targeting protein-protein interaction interfaces. It effectively enables selective and irreversible silencing of a protein, the selectivity being perhaps surprising given that covalent inhibitors have long been maligned for non-selective protein interactions. The key to selectivity here is the helix motif, which directs the ligand specifically to the Bcl2A1 binding site, whereupon a secondary interaction with Cys55 anchors the ligand irreversibly to the protein. As the helix is shortened there is a risk that the initial targeting selectivity could be diminished, but it is worth noting that the majority of protein-protein interactions involving a helix in biology only use 1-4 helical turns.[30d] Therefore, the bicyclic approach shown here may be suitable for recapitulating most protein-helix interactions in biology, with or without a pendant electrophile for enhanced affinity, as long as the helix-

inducing constraints do not negatively impact on binding to the protein target. The inherent ability of the bicyclic helix alone to bind with high affinity to a protein target, without the need for an electrophile, is also demonstrated here for Mcl-1. This example reveals the promise of two adjacent helix constraints[30c,d] for pre-organizing even a short peptide sequence into a receptor-binding helical conformation.[32]

EXPERIMENTAL SECTION

Synthesis. Compounds **1** and FITC-**1** were synthesized and characterized as previously described.[22] Synthetic schemes illustrating the stepwise synthesis of compounds are given in Scheme 1 (compound **5**) and Figure S1 (compound **2-4**, **6-10**) and compound characterization is reported in Supporting Information.

SPPS: assembly of the linear peptide sequence. Peptides were assembled on solid support using Fmoc-based chemistry on a peptide synthesizer (Symphony, Protein Technologies) utilizing a low loading Rink Amide MBHA resin.[22,26] Standard Fmoc-protected amino acids were employed for the synthesis, except: the unusual amino acid Fmoc-(S)-2-(4'-pentenyl)alanine (Fmoc-S_5-OH) was used for the incorporation of the two hydrocarbon handles at positions 1 and 5 and/or positions 9 and 13; the Mtt-protected lysine building block Fmoc-Lys(Mtt)-OH and the OPip-protected aspartic acid Fmoc-Asp(OPip) were used for the incorporation of orthogonally protected Lys/Asp pair at positions 1 and 5 and/or positions 9 and 13; Fmoc-Dap(Mtt)-OH or Fmoc-Dap(Boc)-OH was coupled at the position 2 when appropriate. Usually, 4 equiv. of Fmoc-protected amino acid, 4 equiv. of HCTU and 4 equiv. of DIPEA were used in 2 x 30 min coupling cycles. Fmoc deprotection was achieved by treatment with 1:2 piperidine:DMF for 2 × 3 min. For *N*-terminal acetylated peptides, the N-terminus was

acetylated with Ac_2O:DIPEA (1 M:0.4 M) in DMF for 2 x 5 min. For peptide **9** containing FITC at the *N*-terminus, the peptide assembly continued to incorporate the N-terminal residue Fmoc-βAla-OH prior RCM. FITC was incorporated to the N-terminus by treating the free amine resin with FITC (2 equiv) and DIPEA (4 equiv) in DMF overnight.

On-resin ring closing metathesis (RCM).[25] Prior to RCM, the resin was washed with DCM and dried under high vacuum overnight. The dry resin was then placed in the synthesizer apparatus and swollen in dry DCE under N_2 stream for 10 min and drained. The RCM reaction was performed by treating the resin with a 10 mM solution of Grubbs catalyst 1st generation in dry DCE (2 mL per 50 μmol resin) under N_2 bubbling for 2h. The catalyst solution was drained and a fresh 10 mM Grubbs catalyst solution was added to the resin and reacted for 2h. After that, the resin was washed with DCM and DMF.

On-resin lactam crosslinking. The resin was washed with DCM and treated repeatedly with 2% TFA in DCM (10 x 1 min). After washing with DMF, a solution of PyBOP (4 equiv) and DIPEA (8 equiv) in DMF was added to the resin. Full conversion to the side-chain crosslinked lactam was monitored by the ninhydrin test (usually 4-6 h). After completion, resin was washed with DMF.

On-resin incorporation of the acrylamide or propionamide group to Dap2. After final assembly of the mono- or bis-stapled peptide, the resin was washed with DCM and treated repeatedly with a solution of 2% TFA in DCM (10 x 1 min). After washing with DCM and DMF, the resin was treated with 5% DIPEA in DMF then washed with DMF. After that, a solution of the acid (acrylic acid or propiolic acid; 4 equiv), HATU (4 equiv) and DIPEA (4

equiv) in DMF was added to the resin and the reaction was agitated for 15 min. Finally, the resin was washed with DMF and DCM, dried under vacuum and submitted to cleavage.

Cleavage from solid support and peptide purification. Peptides were cleaved from the resin by treatment with TFA:TIS:H_2O (95:2.5:2.5) for 2 h. The crude peptides were precipitated and washed with cold Et_2O, redissolved in 50% acetonitrile/0.05% TFA in water and lyophilized. Peptides were purified by RP-HPLC using a Phenomenex Luna C18 column eluting at a flow rate of 20 mL/min and a gradient of 20 to 70% buffer B (90% CH_3CN/10% H_2O/0.1% TFA in buffer A, 0.1% TFA in water) over 30 min. Peptides were isolated to purity > 95% as determined by UPLC and RP-HPLC analysis.

Off-resin incorporation of the acrylamide group. After cleavage from resin, the resulting freeze-dried crude peptide was combined with a solution of the acid (acrylic acid; 1.2 equiv), HATU (1.2 equiv) and DIPEA (2.4 equiv) in DMF and the reaction was agitated for 30 min. After that, the reaction was quenched by addition of aqueous TFA and the resulting solution directly injected into the RP-HPLC system for purification (as described above) to give the pure final peptide.

Analytical methods. Purity and identification of the peptides was evaluated by analytical RP-HPLC and UPLC-MS methods. Analytical RP-HPLC was performed on an Agilent system, using a Phenomenex Luna C18 5 um (250 x 4.60 mm) column eluting at a flow rate of 1 mL/min and a gradient of 30 to 100 % buffer B (90% CH_3CN/10% H_2O/0.1% TFA in buffer A, 0.1% TFA in water) over 20 min (Figure S10). UPLC-MS was performed on Shimadzu Nexre UPLC system connected to LCMS-2020 single quadrupole mass spectrometer using an Agilent Zorbax R-ODS III column a gradient of 20 to 80 % buffer B (90% CH_3CN/10% H_2O/0.1% formic acid

in buffer A, 0.1% formic acid in water) over 6 min (Figures S11 and S12). High-resolution mass spectroscopy was carried out on an Applied Biosystems QSTAR Electrospray quadrupole-quadrupole Elite time-of-flight mass spectrometer (Table S2).

Peptide concentration and storage. The concentration of pure peptide samples was determined by NMR in 50% acetonitrile-d_3 in water (1-5 mM) using Pulcon method.[33] Samples were then freeze-dried and redissolved in DMSO (for stock solutions of 10 mM concentration) and stored at -20^{0}C.

Proteins for in vitro binding assays. Bcl-w (ab151806), Bcl-xL (ab 180062), Bcl-2 (ab 84209) and Mcl-1 (ab131682) were purchased from Abcam. A1 (C103) was purchased from Novoprotein. The commercial sample was diluted to a concentration of 10 μM protein in buffer containing 50 mM Tris, 150mM NaCl, 1 mM EDTA and 10 mM TCEP, pH 7.2 and incubated in this TCEP buffer for at least 30 min on an ice bed (max. 60 min) prior to the binding assays.

Fluorescence polarization (FP) binding assays. FP measurements were performed at room temperature using a PHERAstar FS plate reader equipped with fluorescein excitation (490 nm) and emission (520 nm) filters. Samples were placed on a 384-well black plate (Corning) with a total volume in each well of 20 μL with a running buffer containing 50 mM Tris, 150mM NaCl, 1 mM EDTA, 1 mM TCEP, 0.005% Tween-20, pH 7.2. **Direct binding of FBid to Bcl2 proteins.** FBid (5-20 nM, FITC-βAla-DIIRNIARHLAQVGDSMDRSI-NH2)[22] was incubated with different concentrations of each Bcl2 protein (two-fold dilutions ranging from 1 to 1000 nM) in running buffer. FP was measured after 1h incubation and K_d values for Bcl2 protein binding to FBid were determined by nonlinear regression analysis using Prism software 7.0

(GraphPad). The experiment was repeated three times. Results (FBid concentration used/found Kd value): A1 (5/5.8 nM), Mcl-1 (20/105 nM), Bcl-w (10/32.3 nM), Bcl-xL (10/9.7 nM) and Bcl-2 (10/19.8 nM).

Competition assays against FBid/Bcl2 protein complex. The IC_{80} value calculated from the direct binding assay was used to determine the protein concentration to be applied in the competition assays (FBid/protein concentration used: A1 (5/15 nM), Mcl-1 (20/200 nM), Bcl-w (10/65 nM), Bcl-xL (10/60 nM) and Bcl-2 (10/50 nM)). In general, the Bcl2 protein was preincubated with FBid for 30 min in running buffer and combined with a serial dilution of the peptide (ranging from 40 μM to 0.1 nM). After 2 h incubation, fluorescence anisotropy was measured and normalized accordingly to the signals recorded for free FBid (set as 100%) and protein/FBid complex alone (set as 0%). IC_{50} values were determined by nonlinear regression analysis using Prism software 7.0. K_i values (Table S1) were calculated from the observed competitive IC_{50} values after 2 h incubation, the K_d of FBid/Bcl2 protein interaction and known concentrations of labelled peptide and protein using a formula described[34] and available online.[34b] Each experiment was repeated at least three times.

Direct binding of peptide 9 to Bcl2 proteins. Peptide **9** was incubated with different concentrations of each Bcl2 protein (two-fold dilutions starting from 2000 nM) in running buffer. FP was measured after 1 h incubation and K_d values for Bcl2 binding to FBid were determined by nonlinear regression analysis using Prism software 7.0 (GraphPad). The experiment was repeated three times.

Kinetic data for covalent binding of peptides 1-6 to A1. A1 (15 nM) was preincubated with FBid (5 nM) for 30 min in running buffer and combined with a serial dilution of the peptide (at

500, 250, 125, 62.5, 31.2, 15.6, 7.8 and 3.9 nM concentration). After 15, 30, 60, 90 and 120 min incubation, FP was measured and normalized accordingly to the signals recorded for free FBid (set as 100%) and A1/FBid complex alone (set as 0%). The covalent binding was analysed following the methodology described in reference 29. The change in normalized polarization over time (t) was fitted into the equation: normalized polarization = $100*(1 - \exp(-k_{obs}*t))$ and k_{obs} values for each peptide concentration were determined by nonlinear regression analysis (one phase decay) using Prism software 7.0. The calculated k_{obs} values were then used to determine the parameters k_{inact} and K_I by plotting the curve: $k_{obs} = k_{inact}*[peptide]/(K_I + [peptide])$ using Prism software (nonlinear regression, hyperbola equation). Each experiment was repeated at least three times.

SDS-PAGE electrophoresis. A1 and peptides were combined in buffer (50 mM Tris, 150mM NaCl, 1 mM EDTA, 2 mM TCEP, 0.005% Tween-20, pH 7.2) to a final concentration of 1 μM A1 and 10 μM peptide in a total of 20 μL reaction volume. After incubation at room temperature for 2 h, the reaction was immediately submitted to SDS-PAGE analysis as described.[22]

In gel trypsin digestion. Using SDS-PAGE from Figure 5A, the gel band corresponding to the conjugate formed after reacting A1 with peptide **5** was removed and digested with trypsin following a procedure described.[22] The digest was redissolved in 0.5 % formic acid / 50 % acetonitrile and analyzed by LC-MS on a Shimadzu Nexera uHPLC (Japan) coupled to a Triple TOF 5600 mass spectrometer (ABSCIEX, Canada) equipped with a duo electrospray ion source.[22] The data was acquired and processed using Analyst TF 1.6 software (ABSCIEX, Canada). Digested A1 was identified by database searching using ProteinPilot v4 (ABSCIEX) against the UniProt_Sprot_20110925 database. MS-MS spectrum of digested protein was scanned for the inserted peptide sequence ELR sequence from **5** and also for the A1 fragment

sequence LDNVNVVSLDTAR (Figure 4C and S4). A single protein fragment was found and further characterized as the expected conjugated peptide-protein fragment (Figure 5C and S5).

Stability in rat plasma. Peptides **BIM**, **1**, **5** and **8** (5 µL of 1 mM stock solution, dissolved in 5 µL water) were incubated with 490 µL fresh rat plasma over 24 h at 37 °C. During this time, 40 µL aliquots were taken at 0, 0.33, 2, 5, 11 and 22 h and quenched with 120 µL 90% acetonitrile, cooled on ice for 5 min, placed in a centrifuge and spun at 17 g for 10 min. Then, 120 µL of the clear solution was transferred into a vial and analyzed by LC-MS. The rate of peptide deterioration was quantified based on intensity of intact peptide mass peak over time. The experiment was repeated three times for each peptide (Figure S6).

Cells. U937 cells were cultured in RPMI supplemented with 10% FBS, 10 U/mL penicillin, 10 U/mL streptomycin, 2 mM GlutaMax, 2 mM NEAA and 1 mM HEPES. SKMel28 cells were cultured in DMEM supplemented with 10% FBS, 10 U/mL penicillin and 10 U/mL streptomycin.

Covalent binding in live U937 cells. U937 cells were plated at a density of 5 x 10^5 cells and treated with peptides in the presence of 5% FBS for 24 h. After incubation, cells were washed and lysed with Cell Lysis Buffer supplemented with Protease/Phosphatase Inhibitor Cocktail (Cell Signaling Technology). Samples were reduced at 70°C for 5 min followed by western blot analysis using anti-A1 (Cell Signaling Technology) and anti-GAPDH (Sigma Aldrich).

Flow cytometry. SKMel28 cells were treated with 10 µM fluorescein-labeled peptides for 4 h at 37 °C followed by washing and quenching by trypan blue to remove non-specific binding. Cells were then analysed by flow cytometry on a Gallios Flow Cytometer (Becton Dickson) and MFI

data were analyzed using FlowJo (Tree Star Inc). Significant differences were determined using 2-way ANOVA using FITC-BIM as control. P value < 0.0001 ****, 0.001 ***, 0.01 **.

Cell viability and LDH release assay. SKMel28 cells were plated at a density of 4 x 10^4/mL and allowed to adhere overnight. For LDH release assay, peptides were incubated at indicated concentration in serum-free DMEM for 30 min. LDH were measured using CytoTox Non-Radioactive Cytotoxic Assay (Promega) according to manufacturer's instruction. For MTT viability assay, **8** was incubated with or without etoposide at indicated concentration in serum-free DMEM for 48 h. After incubation, MTT (Invitrogen) was then added to the cells at 1 mg/mL for 90 min at 37 °C. The resulting formazan were dissolved in isopropanol and measured using PHERAstar (BMG Labtech) at 570 nm.

Coimmunoprecipitation. SKMel28 cells were treated with **8** (30 μM) for 24 h at 37°C, then lysed with Cell Lysis Buffer supplemented with Protease/Phosphatase Inhibitor Cocktail (Cell Signaling Technology). Immunoprecipitation was performed was per manufacturer's instructions. Briefly, cell lysate was pre-cleared with protein A magnetic beads (Cell Signaling Technology) then incubated overnight with anti-Bim (Cell Signaling Technology). Protein A magnetic beads were then added to form antibody-protein A complex. Unbound proteins were washed in lysis buffer and subjected to boiling to elute proteins. Eluted proteins were used for western blot analysis using anti-Mcl-1 and anti-A1 (Cell Signaling Technology) using iBlot and iBind systems (Invitrogen).

Data analysis. Data were plotted and analyzed using GraphPad Prism 7 for Mac OSX. All values of independent parameters are mean ± SEM of at least three independent experiments. P value < 0.0001 ****, 0.001 ***, 0.01 **.

ASSOCIATED CONTENT

Supporting Information

The Supporting Information is available free of charge on the ACS Publications website.

Additional experimental procedures and figures illustrating peptide synthesis, binding data and stability assays (PDF). A molecular strings file of stapled peptides (CSV).

Corresponding Author Information

* Prof. David P. Fairlie, Institute for Molecular Bioscience, The University of Queensland, Brisbane, QLD 4072, Australia. Email: d.fairlie@imb.uq.edu.au

Author Contributions

A.D.A. synthesized all compounds and performed *in vitro* binding assays. J. L. conducted cell-based assays. K-C. W. performed the LDH assay. A. D. A., R. T. S., A. C. G., Y. X. and D. P. F. designed compounds. A. D. A., R. T. S. and D. P. F. wrote the paper. All authors contributed to editing the paper.

Funding Sources

We thank the National Health and Medical Research Council of Australia (NHMRC) for Senior Principal Research Fellowships to D.F. (1027369, 1117017) and the Australian Research Council for grant support (CE140100011, DP160104442) to D.F.

Acknowledgment

We thank Alun Jones (Institute for Molecular Bioscience, Australia) for assistance with mass spectrometry.

Notes

The authors declare no other competing interests except that R.T.S and A.C.G. are inventors on a patent[23] involving related intellectual property.

Abbreviations

Dap, diaminopropionic acid; DCE, dichloroethane; DCM, dichloromethane; DIPEA, diisopropylethylamine; DMF, dimethylformamide; Fmoc, 9-fluorenylmethyloxy-carbonyl; EDTA, ethylenediaminetetraacetic acid ; FITC, fluorescein isothiocyanate; HATU, 2-(7-Aza-1H-benzotriazol-1-yl)-1,1,3,3-tetramethyluronium hexafluorophosphate; HCTU, 2-(1H-6-chlorobenzotriazol-1-yl)-1,1,3,3-tetramethyluronium hexafluorophosphate; HR-MS, High-resolution mass spectroscopy; MBHA, 4-methyl-benzylhydrylamine; Mtt, 4-methyltrityl; OPip, phenyl isopropyl ester; PyBOP, benzotriazol-1-yl- oxytripyrrolidinophosphonium hexafluorophosphate; RCM, ring-closing metathesis; RP-HPLC, reserved-phase high performance liquid chromatography; TFA, trifluoroacetic acid; TCEP, Tris(2-carboxyethyl)phosphine; TIS, triisopropylsilane.

REFERENCES

1. a) Czabotar, P. E.; Lessene, G.; Strasser, A.; Adams, J. M. Control of apoptosis by the BCL-2 protein family: implications for physiology and therapy. *Nat. Rev. Mol. Cell Biol.* **2014**, *15*, 49-63. b) Ashkenazi, A.; Fairbrother, W. J.; Leverson, J. D.; Souers, A. J. From basic apoptosis discoveries to advanced selective BCL-2 family inhibitors. *Nat. Rev. Drug Discov.* **2017**, *16*, 273-284. c) Hata, A. N.; Engelman, J. A.; Faber, A. C. The BCL2 family: key mediators of the apoptotic response to targeted anticancer therapeutics. *Cancer Discov.* **2015**, *5*, 475-487. d) Dai, H.; Meng, X.; Kaufmann, S. Mitochondrial apoptosis and BH3 mimetics. *F1000Research* **2016**, *5,* 2804.

2. Olin, J. L.; Griffiths, C. L.; Smith, M. B. Venetoclax: A novel B-cell lymphoma-2 inhibitor for chronic lymphocytic leukemia and other hematologic malignancies. *J. Oncol. Pharm. Pract.* **2017**, doi: 10.1177/1078155217718383. Published online: Jan 11, 2017.

3. Beroukhim, R.; Mermel, C. H.; Porter, D.; Wei, G.; Raychaudhuri, S.; Donovan, J.; Barretina, J.; Boehm, J. S.; Dobson, J.; Urashima, M.; Mc Henry, K. T.; Pinchback, R. M.; Ligon, A. H.; Cho, Y.-J.; Haery, L.; Greulich, H.; Reich, M.; Winckler, W.; Lawrence, M. S.; Weir, B. A.; Tanaka, K. E.; Chiang, D. Y.; Bass, A. J.; Loo, A.; Hoffman, C.; Prensner, J.; Liefeld, T.; Gao, Q.; Yecies, D.; Signoretti, S.; Maher, E.; Kaye, F. J.; Sasaki, H.; Tepper, J. E.; Fletcher, J. A.; Tabernero, J.; Baselga, J.; Tsao, M.-S.; Demichelis, F.; Rubin, M. A.; Janne, P. A.; Daly, M. J.; Nucera, C.; Levine, R. L.; Ebert, B. L.; Gabriel, S.; Rustgi, A. K.; Antonescu, C. R.; Ladanyi, M.; Letai, A.; Garraway, L. A.; Loda, M.; Beer, D. G.; True, L. D.; Okamoto, A.; Pomeroy, S. L.; Singer, S.; Golub, T. R.; Lander, E. S.; Getz, G.; Sellers, W. R.; Meyerson, M. The landscape of somatic copy-number alteration across human cancers. *Nature* **2010**, *463*, 899-905.

4. Vogler, M. BCL2A1: the underdog in the BCL2 family. *Cell Death Differ.* **2012**, *19*, 67-74.

5. Hind, C. K.; Carter, M. J.; Harris, C. L.; Chan, H. T. C.; James, S.; Cragg, M. S. Role of the pro-survival molecule Bfl-1 in melanoma. *Int. J. Biochem. Cell Biol.* **2015**, *59*, 94-102.

6. Senft, D.; Berking, C.; Graf, S. A.; Kammerbauer, C.; Ruzicka, T.; Besch, R. Selective induction of cell death in melanoma cell lines through targeting of Mcl-1 and A1. *PloS One* **2012**, *7*, e30821.

7. Haq, R.; Yokoyama, S.; Hawryluk, E. B.; Jönsson, G. B.; Frederick, D. T.; McHenry, K.; Porter, D.; Tran, T.-N.; Love, K. T.; Langer, R.; Anderson, D. G.; Garraway, L. A.; Duncan, L. M.; Morton, D. L.; Hoon, D. S. B.; Wargo, J. A.; Song, J. S.; Fisher, D. E., BCL2A1 is a lineage-specific antiapoptotic melanoma oncogene that confers resistance to BRAF inhibition, *Proc. Natl. Acad. Sci. U.S.A.* **2013**, *110*, 4321-4326.

8. Fofaria, N. M.; Frederick, D. T.; Sullivan, R. J.; Flaherty, K. T.; Srivastava, S. K. Overexpression of Mcl-1 confers resistance to BRAF(V600E) inhibitors alone and in combination with MEK1/2 inhibitors in melanoma. *Oncotarget* **2015**, *6*, 40535-40556.

9. Chen, L.; Fletcher, S. Mcl-1 inhibitors: a patent review. *Expert Opin. Ther. Pat.* **2017**, *27*, 163-178.

10. Kotschy, A.; Szlavik, Z.; Murray, J.; Davidson, J.; Maragno, A. L.; Le Toumelin-Braizat, G.; Chanrion, M.; Kelly, G. L.; Gong, J.-N.; Moujalled, D. M.; Bruno, A.; Csekei, M.; Paczal, A.; Szabo, Z. B.; Sipos, S.; Radics, G.; Proszenyak, A.; Balint, B.; Ondi, L.; Blasko, G.; Robertson, A.; Surgenor, A.; Dokurno, P.; Chen, I.; Matassova, N.; Smith, J.; Pedder, C.; Graham, C.; Studeny, A.; Lysiak-Auvity, G.; Girard, A.-M.; Gravé, F.; Segal, D.; Riffkin, C. D.; Pomilio, G.; Galbraith, L. C. A.; Aubrey, B. J.; Brennan, M. S.; Herold, M. J.; Chang, C.; Guasconi, G.; Cauquil, N.; Melchiore, F.; Guigal-Stephan, N.; Lockhart, B.; Colland, F.; Hickman, J. A.; Roberts, A. W.; Huang, D. C. S.; Wei, A. H.; Strasser, A.; Lessene, G.; Geneste, O. The MCL1 inhibitor S63845 is tolerable and effective in diverse cancer models. *Nature* **2016**, *538*, 477-482.

11. a) Stewart, M. L.; Fire, E.; Keating, A. E.; Walensky, L. D. The MCL-1 BH3 helix is an exclusive MCL-1 inhibitor and apoptosis sensitizer. *Nat. Chem. Biol.* **2010**, *6*, 595-601. b) Muppidi, A.; Doi, K.; Edwardraja, S.; Drake, E. J.; Gulick, A. M.; Wang, H.-G.; Lin, Q. Rational design of proteolytically stable, cell-permeable peptide-based selective Mcl-1 Inhibitors. *J. Am. Chem. Soc.* **2012***, 134*, 14734-14737.

12. Dutta, S.; Chen, T. S.; Keating, A. E. Peptide ligands for pro-survival protein Bfl-1 from computationally guided library screening. *ACS Chem. Biol.* **2013**, *8*, 778-788.

13. Jenson, J. M.; Ryan, J. A.; Grant, R. A.; Letai, A.; Keating, A. E. Epistatic mutations in PUMA BH3 drive an alternate binding mode to potently and selectively inhibit anti-apoptotic Bfl-1. *Elife* **2017**, *6*, e25541.

14. Herman, M. D.; Nyman, T.; Welin, M.; Lehtiö, L.; Flodin, S.; Trésaugues, L.; Kotenyova, T.; Flores, A.; Nordlund, P. Completing the family portrait of the anti-apoptotic Bcl-2 proteins: Crystal structure of human Bfl-1 in complex with Bim. *FEBS Letters* **2008**, *582*, 3590-3594.

15. Delgado-Soler, L.; Pinto, M.; Tanaka-Gil, K.; Rubio-Martinez, J. Molecular determinants of Bim(BH3) peptide binding to pro-survival proteins. *J. Chem. Inf. Model.* **2012**, *52*, 2107-2118.

16. Boersma, M. D.; Sadowsky, J. D.; Tomita, Y. A.; Gellman, S. H. Hydrophile scanning as a complement to alanine scanning for exploring and manipulating protein–protein recognition: Application to the Bim BH3 domain. *Prot. Sci.* **2008**, *17*, 1232-1240.

17. Lee, E. F.; Czabotar, P. E.; van Delft, M. F.; Michalak, E. M.; Boyle, M. J.; Willis, S. N.; Puthalakath, H.; Bouillet, P.; Colman, P. M.; Huang, D. C. S.; Fairlie, W. D. A novel BH3 ligand that selectively targets Mcl-1 reveals that apoptosis can proceed without Mcl-1 degradation. *J. Cell Biol.* **2008**, *180*, 341-355.

18. Zhang, S.; Link, A. J. Bcl-2 family interactome analysis using bacterial surface display. *Integr. Biol.* **2011***, 3*, 823-831.

19. Fire, E.; Gullá, S. V.; Grant, R. A.; Keating, A. E., Mcl-1–Bim complexes accommodate surprising point mutations via minor structural changes. *Prot. Sci.* **2010,** *19*, 507-519.

20. LaBelle, J. L.; Katz, S. G.; Bird, G. H.; Gavathiotis, E.; Stewart, M. L.; Lawrence, C.; Fisher, J. K.; Godes, M.; Pitter, K.; Kung, A. L.; Walensky, L. D. A stapled BIM peptide overcomes apoptotic resistance in hematologic cancers. *J. Clin. Invest.* **2012**, *122*, 2018-2031.

21. Rezaei Araghi, R.; Bird, G. H.; Ryan, J. A.; Jenson, J. M.; Godes, M.; Pritz, J. R.; Grant, R. A.; Letai, A.; Walensky, L. D.; Keating, A. E., Iterative optimization yields Mcl-1–targeting stapled peptides with selective cytotoxicity to Mcl-1–dependent cancer cells. *Proc. Natl. Acad. Sci. U.S.A.* **2018,** *115*, E886-E895.

22. de Araujo, A. D.; Lim, J.; Good, A. C.; Skerlj, R. T.; Fairlie, D. P. Electrophilic helical peptides that bond covalently, irreversibly and selectively in a protein-protein interaction site, *ACS Med. Chem. Lett.* **2017**, *8*, 22-26.

23. Skerlj, R.; Good, A. Peptidomimetic Compounds. U.S. Patent, 9,493,510, Nov 15, 2016.

24. a) Huhn, A. J.; Guerra, R. M.; Harvey, E. P.; Bird, G. H.; Walensky, L. D. Selective covalent targeting of anti-apoptotic BFL-1 by cysteine-reactive stapled peptide inhibitors. *Cell Chem. Biol.* **2016**, *23*, 1123-1134. b) Harvey, E. P.; Seo, H.-S.; Guerra, R. M.; Bird, G. H.; Dhe-Paganon, S.; Walensky, L. D. Crystal structures of anti-apoptotic Bfl-1 and its complex with a covalent stapled peptide inhibitor. *Structure* **2018,** *26*, 153-160.e4. c) Barile, E.; Marconi, G. D.; De, S. K.; Baggio, C.; Gambini, L.; Salem, A. F.; Kashyap, M. K.; Castro, J. E.; Kipps, T. J.; Pellecchia, M., hBfl-1/hNOXA interaction studies provide new insights on the role of Bfl-1 in cancer cell resistance and for the design of novel anticancer agents. *ACS Chem. Biol.* **2017,** *12*, 444-455.

25. Verdine, G. L.; Hilinski, G. J. Stapled Peptides for Intracellular Drug Targets. In *Methods in Enzymology*; Wittrup, K. D., Gregory, L. V., Eds.; Academic Press: New York, 2012; Vol. 503, pp 3-33.

26. de Araujo, A. D.; Hoang, H. N.; Kok, W. M.; Diness, F.; Gupta, P.; Hill, T. A.; Driver, R. W.; Price, D. A.; Liras, S.; Fairlie, D. P. Comparative alpha helicity of cyclic pentapeptides in water. *Angew. Chem. Int. Ed.* **2014***, 53*, 6965-6969.

27. Hoang, H. N.; Driver, R. W.; Beyer, R. L.; Hill, T. A.; D. de Araujo, A.; Plisson, F.; Harrison, R. S.; Goedecke, L.; Shepherd, N. E.; Fairlie, D. P. Helix nucleation by the smallest known α-helix in water. *Angew. Chem. Int. Ed.* **2016**, *55*, 8275-8279.

28. Vougioukalakis, G. C.; Grubbs, R. H. Ruthenium-based heterocyclic carbene-coordinated olefin metathesis catalysts. *Chem. Rev.* **2010,** *110*, 1746-1787.

29. Strelow, J. M. A perspective on the kinetics of covalent and irreversible inhibition. *SLAS Discov.* **2017**, *22*, 3-20.

30. a) Reid, R. C.; March, D. R.; Dooley, M. J.; Bergman, D. A.; Abbenante, G.; Fairlie, D. P. A novel bicyclic enzyme inhibitor as a consensus peptidomimetic for the receptor-bound conformations of 12 peptidic inhibitors of HIV-1 protease. *J. Am. Chem. Soc.* **1996***, 118*, 8511-8517. b) Fairlie, D. P.; Tyndall, J. D. A.; Reid, R. C.; Wong, A. K.; Abbenante, G.; Scanlon, M. J.; March, D. R.; Bergman, D. A.; Chai, C. L. L.; Burkett, B. A. Conformational selection of inhibitors and substrates by proteolytic enzymes: implications for drug design and polypeptide processing. *J. Med. Chem.* **2000**, *43*, 1271-1281. c) Shepherd, N. E.; Abbenante, G.; Fairlie, D. P. Consecutive cyclic pentapeptide modules form short α-helices that are very stable to water and denaturants. *Angew. Chem. Int. Ed.* **2004**, *43*, 2687-2690. d) Harrison, R. S.; Shepherd, N. E.; Hoang, H. N.; Ruiz-Gómez, G.; Hill, T. A.; Driver, R. W.; Desai, V. S.; Young, P. R.; Abbenante, G.; Fairlie, D. P. Downsizing human, bacterial, and viral proteins to short water-stable alpha helices that maintain biological potency. *Proc. Natl. Acad. Sci. U.S.A.* **2010***, 107*, 11686-11691.

31. a) Sanderson, P. E. J. Small, noncovalent serine protease inhibitors. *Med. Res. Rev.* **1999**, *19*, 179-197. b) Leung, D.; Abbenante, G.; Fairlie, D. P. Protease inhibitors: current status and future prospects. *J. Med. Chem.* **2000**, *43*, 305-341.

32. Hill, T. A.; Shepherd, N. E.; Diness, F.; Fairlie, D. P., Constraining cyclic peptides to mimic protein structure motifs. *Angew. Chem. Int. Ed.* **2014,** *53*, 13020-13041.

33. Wider, G.; Dreier, L. Measuring protein concentrations by NMR spectroscopy. *J. Am. Chem. Soc.* **2006**, *128*, 2571-2576.

34. a) Nikolovska-Coleska, Z.; Wang, R.; Fang, X.; Pan, H.; Tomita, Y.; Li, P.; Roller, P. P.; Krajewski, K.; Saito, N. G.; Stuckey, J. A.; Wang, S. Development and optimization of a binding assay for the XIAP BIR3 domain using fluorescence polarization. *Anal. Biochem.* **2004**, *332*, 261-273. b) Online tool to calculate Ki for fluorescence-based competitive binding assays available at: http://sw16.im.med.umich.edu/software/calc_ki/ (accessed Feb 27, 2018).

TABLE OF CONTENTS